

AD-A042 433

AEROSPACE CORP EL SEGUNDO CALIF CHEMISTRY AND PHYSICS LAB F/G 22/2
SPACECRAFT CONTAMINATION UNDER SIMULATED ORBITAL ENVIRONMENT.(U)
JUL 77 R W PHILLIPS, L U TOLENTINO F04701-76-C-0077

UNCLASSIFIED

TR-0077(2270-30)-2

SAMSO-TR-77-130

NL

| OF |
AD
A042433



AD A 042433

Spacecraft Contamination Under Simulated Orbital Environment

Chemistry and Physics Laboratory
The Ivan A. Getting Laboratories
The Aerospace Corporation
El Segundo, Calif. 90245

6 July 1977

Interim Report

APPROVED FOR PUBLIC RELEASE;
DISTRIBUTION UNLIMITED

Prepared for
SPACE AND MISSILE SYSTEMS ORGANIZATION
AIR FORCE SYSTEMS COMMAND
Los Angeles Air Force Station
P.O. Box 92960, Worldway Postal Center
Los Angeles, Calif. 90009

AD No. _____
DDC FILE COPY

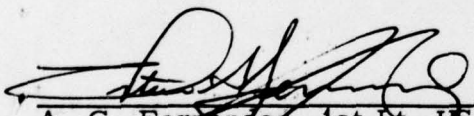
[Handwritten signature] (12)

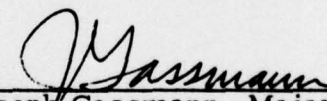
DDC
AUG 4 1977
C

This interim report was submitted by The Aerospace Corporation, El Segundo, CA 90245, under Contract No. F04701-76-C-0077 with the Space and Missile Systems Organization, Deputy for Advanced Space Programs, P.O. Box 92960, Worldway Postal Center, Los Angeles, CA 90009. It was reviewed and approved for The Aerospace Corporation by S. Siegel, Director, Chemistry and Physics Laboratory. Lieutenant A. G. Fernandez, SAMSO/YAPT, was the project officer for Advanced Space Programs.

This report has been reviewed by the Information Office (OI) and is releasable to the National Technical Information Service (NTIS). At NTIS, it will be available to the general public, including foreign nations.

This technical report has been reviewed and is approved for publication. Publication of this report does not constitute Air Force Approval of the report's findings or conclusions. It is published only for the exchange and stimulation of ideas.


A. G. Fernandez, 1st Lt, USAF
Project Officer


Joseph Gassmann, Major, USAF

FOR THE COMMANDER


LEONARD E. BALTZELL, Col, USAF, Asst.
Deputy for Advanced Space Programs

ACCESSION for ☒ Wire Section ☐
NTIS ☐ Bitt Section ☐
DDC
UNANNOUNCED
JUSTIFICATION
BY DISTRIBUTION/AVAILABILITY CODES
Dist. ☐ ☐ ☐ ☐
A

UNCLASSIFIED

SECURITY CLASSIFICATION OF THIS PAGE (When Data Entered)

REPORT DOCUMENTATION PAGE		READ INSTRUCTIONS BEFORE COMPLETING FORM
1. REPORT NUMBER SAMS0-TR-77-130	2. GOVT ACCESSION NO.	3. RECIPIENT'S CATALOG NUMBER
4. TITLE (and Subtitle) SPACECRAFT CONTAMINATION UNDER SIMULATED ORBITAL ENVIRONMENT.	5. TYPE OF REPORT & PERIOD COVERED Interim report	
7. AUTHOR(s) Roger W. Phillips, Lucio U. Tolentino, and Seymour Feuerstein	6. PERFORMING ORG. REPORT NUMBER TR-0077(2270-30)-2	
9. PERFORMING ORGANIZATION NAME AND ADDRESS The Aerospace Corporation El Segundo, Calif. 90245	8. CONTRACT OR GRANT NUMBER(s) F04701-76-C-0077	
11. CONTROLLING OFFICE NAME AND ADDRESS Space and Missile Systems Organization Air Force Systems Command Los Angeles, Calif. 90009	10. PROGRAM ELEMENT, PROJECT, TASK AREA & WORK UNIT NUMBERS	
14. MONITORING AGENCY NAME & ADDRESS (if different from Controlling Office)	12. REPORT DATE 6 July 1977	
	13. NUMBER OF PAGES 44	
	15. SECURITY CLASS. (of this report) Unclassified	
	15a. DECLASSIFICATION/DOWNGRADING SCHEDULE	
16. DISTRIBUTION STATEMENT (of this Report) Approved for public release; distribution unlimited		
17. DISTRIBUTION STATEMENT (of the abstract entered in Block 20, if different from Report) <div style="text-align: right;"> DDC APPROVED AUG 4 1977 RECEIVED C </div>		
18. SUPPLEMENTARY NOTES		
19. KEY WORDS (Continue on reverse side if necessary and identify by block number) Contamination RTV-615 Volatile Condensable Material (VCM) RTV-566 Space Simulation Facility Kapton Multiple Internal Reflection Spectroscopy		
20. ABSTRACT (Continue on reverse side if necessary and identify by block number) Volatile condensable material (VCM) measurements on a number of spacecraft materials have indicated that contamination rates onto surfaces at subambient temperatures cannot be predicted from standard outgassing tests, particularly where long-term exposures are involved. Contamination rates may depend markedly on temperature differentials between source and collector, the collection temperature, the source geometry and the exposure time. Contamination rates may also be influenced by solar irradiation. The results of this study were obtained on a new VCM facility that overcomes →		

DD FORM 1473
(FACSIMILE)

409383

UNCLASSIFIED

SECURITY CLASSIFICATION OF THIS PAGE (When Data Entered)

UNCLASSIFIED

SECURITY CLASSIFICATION OF THIS PAGE(When Data Entered)

19 KEY WORDS (Continued)

(1 to 10 nanotorr)

20 ABSTRACT (Continued)

cont → many deficiencies experienced in earlier designs and permits accurate simulation of space environmental conditions. Advantages of the present system include an oil-free, high-vacuum chamber (10^{-8} - 10^{-9} torr), source temperatures from ambient to 125°C, collection temperatures from -140°C to +125°C, total mass-loss measurements, in-situ VCM mass measurements with use of an internal-temperature-compensated quartz-crystal microbalance, in-situ vacuum ultraviolet irradiation of either the specimen or of the collected VCM, and infrared identification of the VCM by multiple internal reflection spectroscopy. The system also features automated data acquisition and data processing.

↑

UNCLASSIFIED

SECURITY CLASSIFICATION OF THIS PAGE(When Data Entered)

PREFACE

The authors wish to thank Dr. P. D. Fleischauer and D. F. Hall for their critical reviews, which aided in clarification of the text. We also wish to thank R. D. Brink for significant contributions to the early design of the VCM facility and W. J. Kalinowski for invaluable assistance in interfacing the data acquisition system to the VCM facility.

CONTENTS

PREFACE	1
I. INTRODUCTION	7
II. INSTRUMENTATION	9
A. Chamber	9
B. Collection Apparatus	9
C. Temperature Controls	14
D. Vacuum Ultraviolet Sources	14
E. Microprocessor Data Acquisition System	16
F. Transfer Vessel	17
III. EXPERIMENTAL	19
A. Materials and Sample Preparation	19
B. Procedure	19
IV. THEORETICAL CONSIDERATIONS	23
V. RESULTS AND DISCUSSION	31
A. Volatile Condensable Material and Total Mass Loss	31
B. Radiation Effects	37
C. VCM Identification	40
VI. CONCLUSIONS	45
REFERENCES	47

FIGURES

1.	Block diagram of VCM facility	10
2.	VCM facility	11
3.	Double quartz crystal microbalance (DQCM)	12
4.	Collection apparatus	15
5.	Geometrical considerations for solving relationship of M_T to M_p	24
6.	Geometrical considerations for solving relationship of mass on DQCM to M_T when source and collectors are nonparallel	26
7.	Geometrical considerations for solving relationship of mass on DQCM when source is large relative to collector-source distance	27
8.	VCM deposition profiles of RTV-615	35
9.	VCM deposition profile of RTV-615 when collectors were irradiated by VUV	39
10.	Infrared spectra (25°C) of RTV-615 VCM and RTV-615 parent material	41

TABLES

1.	VCM Facility Outgassing Conditions	21
2.	Outgassing Results	32
3.	Selected Data from SRI VCM Tests	36

I. INTRODUCTION

In order to carry out their assigned missions, satellites must not only function with very high reliability, they must continue to do so for long periods of time. As time passes, the prevention of contamination on critical thermal control and optical surfaces becomes more difficult. In some applications, a small change in the solar absorptance, α_s , due to contaminant effects can seriously hamper the performance of a mission. It is essential, therefore, that the importance of various sources of contamination be ascertained in order that corrective action can be initiated. Recent flight data indicate that the contamination problem is still significant.¹

A number of spacecraft programs have thermal control surfaces that must operate at cryogenic temperatures and may be in direct line of sight with contamination sources. Even surfaces out of direct line of sight of outgassing material may receive condensate.² Extrapolation of room temperature collection data to cryogenic conditions is difficult, particularly if long-term exposure effects are sought. Accurate measurements of contamination under conditions that simulate long-term orbital environments are particularly needed to estimate operational lifetimes for satellites with critical surfaces operating at cryogenic temperatures.

Since problems caused by contaminant films on critical surfaces were first discovered, numerous studies have been carried out to determine the outgassing properties of spacecraft materials.³⁻⁷ The standard method of determining the acceptability of a candidate spacecraft material is to heat

the sample in vacuum at 125° C for 24 hours.³⁻⁵ It has been proposed that the total mass loss and the material depositing on a 25° C surface from this heated source be less than 1% and 0.1%, respectively, of the original sample mass. This method is excellent for the rapid screening of materials proposed for spacecraft use, but rates of outgassing and condensation cannot be determined. A calibrated microbalance system has been developed that allows the measurement of outgassing rate either isothermally or with a monotonic increase in temperature.⁶ However, the rate of condensation or possible re-evaporation of the condensate cannot be measured. Another system provides more information by continuously monitoring the mass loss of the material as well as the mass gain of the condensate.⁷ In addition, reflectance and scattering measurements of the contaminated surfaces are obtained. Unfortunately, no provision is available for identifying the contamination, and the system suffers from a non-line-of-sight configuration between source and collector. The above systems also have one or more of the following additional disadvantages; they are not oil free, outgassing occurs during evacuation, cryogenic collection of VCM is not possible, and they do not provide for in-situ simulated solar irradiation of either the source or the collector.

In this paper, a new automated space simulation facility that overcomes most of the cited deficiencies of earlier designs is described. Measurements are discussed, and the results of a number of outgassing experiments carried out on this facility are analyzed.

II. INSTRUMENTATION

A. CHAMBER

The VCM apparatus (Figs. 1 and 2) is an oil-free stainless steel vacuum chamber that is pumped by a liquid-nitrogen-cooled molecular sieve sorption pump and a Perkin-Elmer/Ultek 100 l/sec ion pump. There are no polymeric sealants or insulation within the chamber. Seals are made with copper gaskets and glass-to-metal seals; electrical insulation is achieved by encircling bare copper wire with ceramic beads. In contrast to previous systems, a tubular cryoshield at -196°C extends around the outgassing source (the specimen) and up to just in front of the collectors. This arrangement restricted the experiments to measuring only line-of-sight contamination.² Demand of liquid nitrogen through the cryoshield was controlled by a novel two-tank sequencer.⁸

B. COLLECTION APPARATUS

1. DOUBLE QUARTZ CRYSTAL MICROBALANCE (DQCM)

The mass sensing element is a 1.5-in. \times 0.75-in. single crystal wafer of quartz, resonating at 5 MHz, of the type developed by Termeulen, et al.⁹ Approximately 50 Å of chromium, followed by 3000 Å of gold, is vacuum deposited onto the quartz to form the collecting and reference electrodes, as shown in Fig. 3. Resonance across both reference and collector sides of the quartz crystal is induced by a Miller oscillator in conjunction with a mixer-amplifier output circuit. In operation, the collector side of the crystal is exposed to mass deposition, whereas the reference side is protected

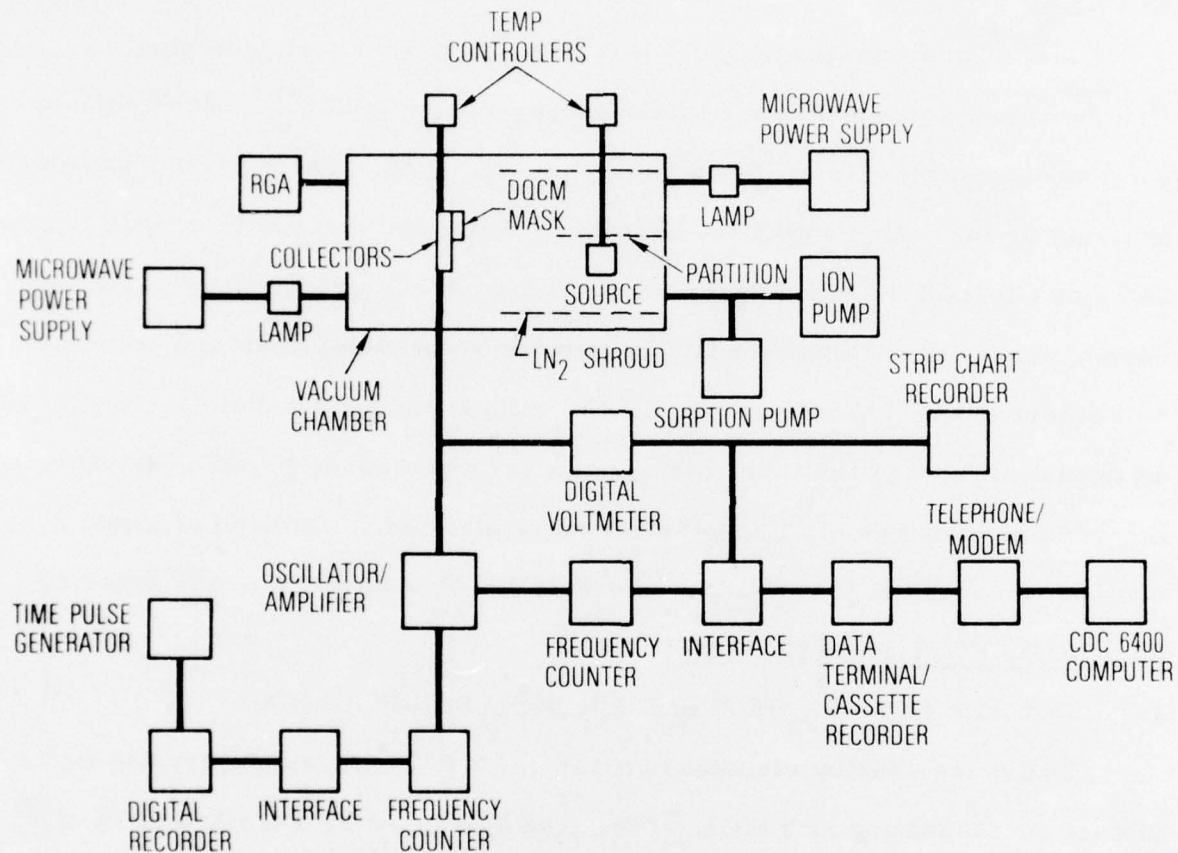


Figure 1. Block diagram of VCM facility

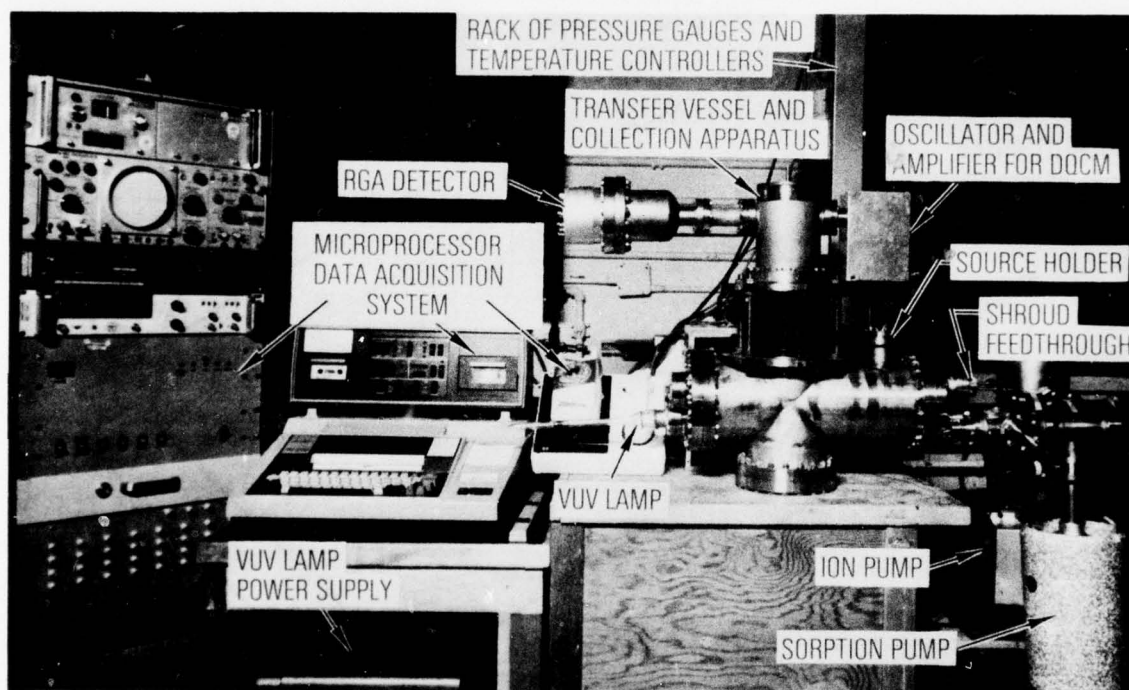


Figure 2. VCM facility

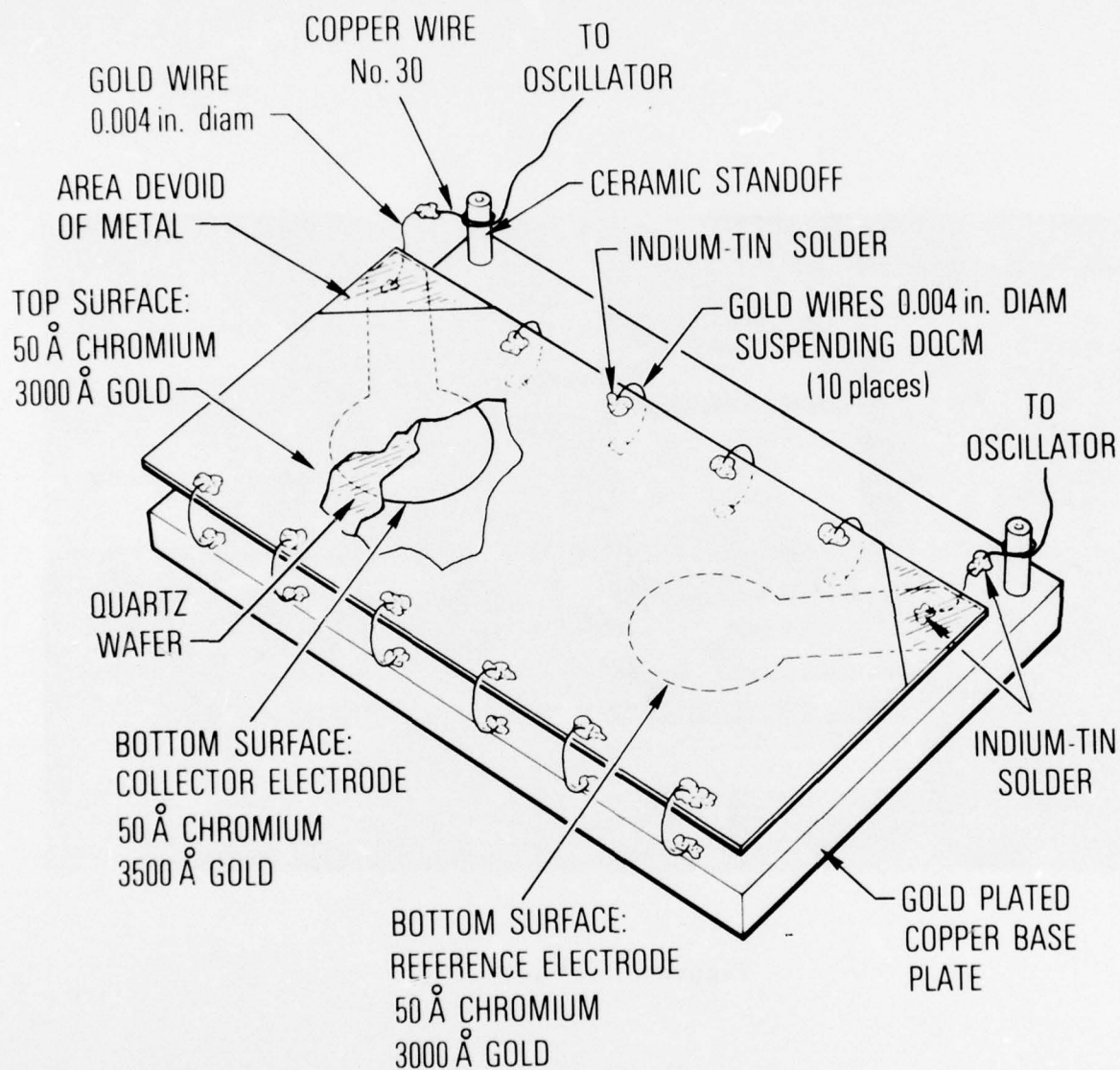


Figure 3. Double quartz crystal microbalance (DQCM)

from mass deposition by a mask. It is important to make the collecting electrode more massive than the reference electrode in order to avoid crystal frequency instabilities. Apparently, the active portions of the two crystals have a strong tendency to mechanically couple in the regime of near mass equivalence. An additional 500 Å of gold deposited on the collector side of the crystal is generally sufficient to overcome this problem.

The quartz is suspended from an oxygen free high-conductivity (OFHC) copper baseplate by using 0.004 in. diam gold wire, soldered to the front face with indium. Such a mounting minimizes mechanical damping and crystal stress caused by differential thermal contractions.

Two types of AT-cut crystals were used in the present study, one cut at 35° 10' and the other at 39° 49'. Beat frequency profiles over temperatures of -140 to 25°C showed small shifts that amounted to 30 Hz and 200 Hz, respectively. Absolute shifts were on the order of 13 kHz. These low beat frequency shifts indicate, in effect, that this type of crystal monitor has good inherent temperature compensation. Normally, two crystals must be mounted independently in the same vicinity in order to achieve similar temperature compensation.

Vacuum-evaporated aluminum films of various thicknesses on the monitoring side of the crystal yielded an average mass sensitivity of $58.6 \text{ Hz-}\mu\text{g}^{-1}\text{-cm}^2$, which is in reasonable agreement with the theoretical value of $57.5 \text{ Hz-}\mu\text{g}^{-1}\text{-cm}^2$ for an AT-cut 5 MHz quartz crystal.¹⁰

2. INTERNAL REFLECTANCE ELEMENT (IRE)

A trapezoidal 45° cut KRS-5 internal reflectance element serves as a collecting substrate for infrared (IR) identification of the condensate. It is located immediately below the quartz crystal microbalance Fig. 4. Infrared spectra were taken after each test, at ambient conditions, on a Perkin Elmer IR spectrometer (Model 467) equipped with a IRE holder accessory.

3. RESIDUAL GAS ANALYZER (RGA)

A quadrupole residual gas analyzer (Electronic Associates Model Quad 200) is also used for mass identification of the outgassing material (Fig. 1).

C. TEMPERATURE CONTROLS

The outgassing source (specimen) holder and the base to which the collectors are attached are made of copper for rapid and uniform temperature accommodation. Source temperatures can be set at -196°C or adjusted between 25 and 125°C with a cartridge heater in conjunction with an API (Model 503K) temperature controller (API Company) and an iron-constantan thermocouple. Temperature control of the collectors can be maintained between -140 and +125°C by controlled heating of the cooled copper base. Heat conduction prevents lower temperatures at the collectors. The collectors and cryoshield temperatures are monitored by copper-constantan thermocouples referenced to a junction at 77°K.

D. VACUUM ULTRAVIOLET SOURCES

Mercury vacuum ultraviolet lamps with Suprasil windows are attached to the test chamber such that either the condensate or the specimen can be

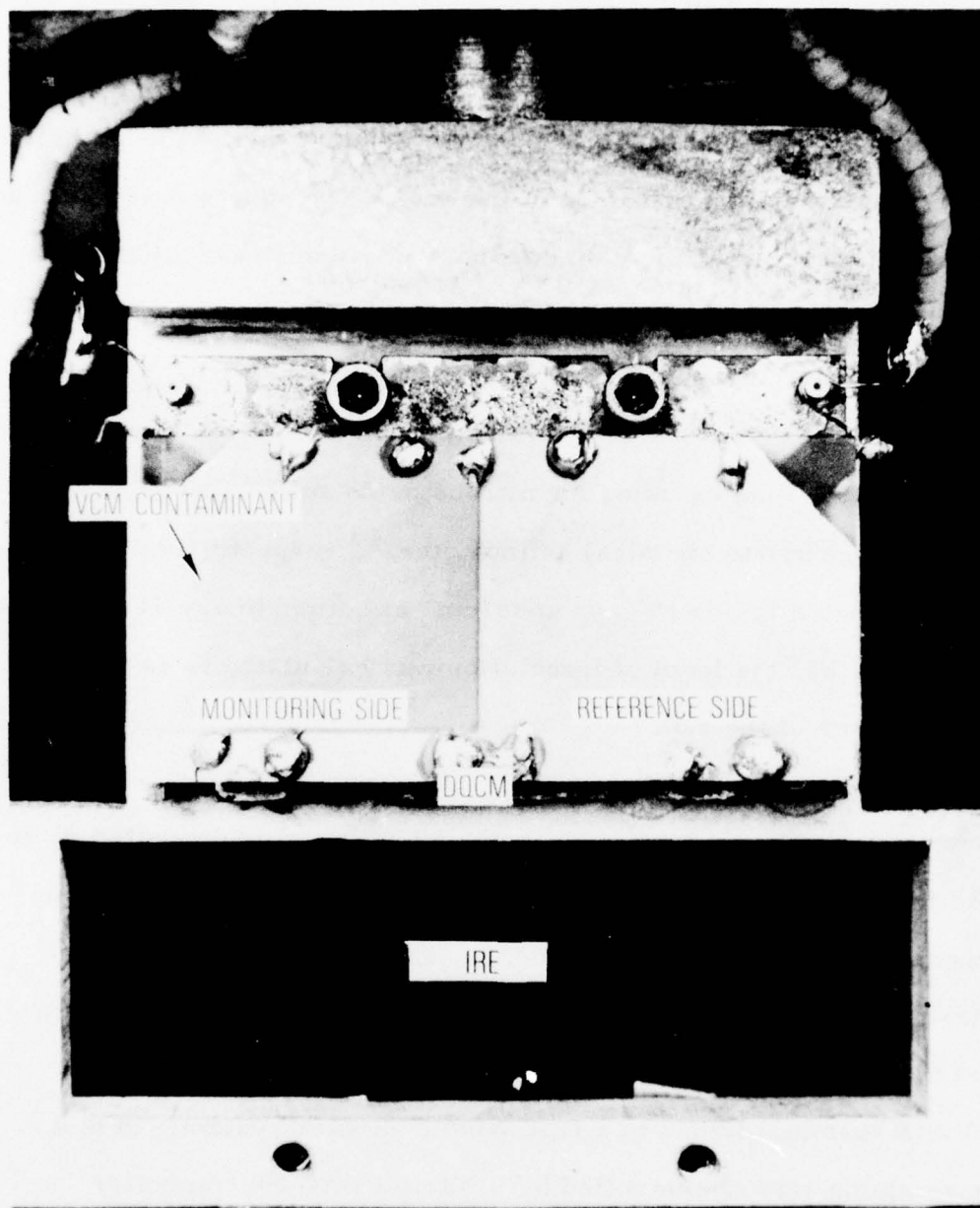


Figure 4. Collection apparatus

irradiated in situ. Power to the lamps is supplied by a Raytheon PGM 10X1 microwave power (2.45 GHz) supply with a "C" type antenna. The partition prevents direct ultraviolet irradiation of the outgassing source during condensate irradiation. Similarly, the collector base prevents irradiation of the condensate during specimen irradiation. It is necessary to properly shield the rf antenna in order to prevent oscillator instabilities.

The photon flux at a distance of 27.9 cm from the source was measured at $\lambda = 184.9$ and 253.7 nm by using the nitrous oxide actinometer¹¹⁻¹² and the potassium ferrioxylate chemical actinometer,¹³ respectively. Flux densities were calculated to be $\approx 10^{14}$ photons/cm² at both primary wavelengths. At these wavelengths, the level of irradiation was calculated to be about 3.1 times the power of the sun.¹⁴

E. MICROPROCESSOR DATA ACQUISITION SYSTEM

Changes in the DQCM beat frequencies as material is deposited or re-evaporated from the unmasked side of the crystal is displayed on a Heath digital frequency counter (Model SM-104A). The frequency data are recorded directly by a digital printer, or indirectly onto a cassette tape for permanent storage. Direct recording is done with a Texas Instruments Silent 700 ASR terminal linked to a CDC 6400 computer system. In this case, the sampling rate is controlled by a Varitel DAC-80 controller coupled to a NLS multichannel scanner. Alternatively, a Hewlett Packard (Model 562A) printer can be used to obtain an immediate hard copy of the frequency data. Here, the data are subsequently key punched and batched through a CDC 7600 computer. Disk files within the CDC 7600 system are

also created to permit manipulation of the data into final form and to permit plotting by a multiten Cal-Comp plotter. For the latter acquisition system, a specially built pulse unit controls the data sampling interval from 1 sec to 1 hr. A 10 min time interval proved to be most convenient. The time pulse generator was protected from transient line signals by using an isolation transformer.

F. TRANSFER VESSEL

A large metal bellows located on the top side of the vacuum chamber is designed for ex-situ ultraviolet and visible spectral measurements of the condensate under actual collecting conditions, i. e., low temperature and vacuum. By the compression of the bellows, the collector assembly passes into a latching cover in the base of the chamber. An indium gasket serves as a seal. When the latches are in place, the entire assembly, including the cover (with appropriate optical windows), can be removed from the system after the rest of the chamber has been back-filled with dry nitrogen. This particular feature was not used in this investigation.

III. EXPERIMENTAL

A. MATERIALS AND SAMPLE PREPARATION

The RTV-615 samples, polydimethylsiloxane from General Electric, were prepared in disk form according to aerospace industry standards by mixing 90.9 wt % RTV-615A polymer and 9.09 wt % RTV-615B curing agent.

The RTV-566 sample, polymethylphenylsiloxane from General Electric, was prepared according to aerospace standards by mixing 99.8 wt % RTV-566A polymer and 0.2 wt % RTV-566B curing agent.

The Kapton sample, a 3-mil polyimide film, was used as-received from the manufacturer, DuPont Corp.

Samples were cured in a desiccator at room temperature for seven days. No effort was made to precondition the samples for humidity and temperature prior to use. The RTV samples were cast directly into a copper mold of disk design and attached directly to the copper specimen holder. The Kapton film was cut to disk size and kept in place by a fastened wire screen.

B. PROCEDURE

Prior to each experiment, the system was baked at 125°C for 48 hr. A vacuum of 10^{-8} to 10^{-9} torr was ultimately achieved. With the cryogenic shroud at -196°C, background contamination rates were reduced to negligible amounts, $\leq 0.25 \text{ pg-cm}^{-2}\text{-min}^{-1}$, as measured by the frequency of the DQCM at -140°C.

Specimens were attached to the sample holder and fixed into place after first closing off the pumping system and backfilling the chamber with dry

nitrogen. Sorption pumping for approximately 10 min reduced the chamber pressure to $\approx 10^{-4}$ torr, after which the sample was frozen to -196°C . This freezing procedure was necessary in order to prevent premature outgassing. At this point, the chamber was switched from sorption pumping to ion pumping. The cryogenic shroud, the DQCM, and the IRE were then cooled to their respective temperatures.

Once the vacuum had been attained and the system temperature equilibrated, the source was heated to the desired temperature as rapidly as possible. Equilibrium source temperature was achieved in a matter of minutes. The total mass of material collecting on the DQCM was measured every 10 min by automatically recording the DQCM beat frequency. Total collection time varied from 1 to 5 days. Irradiations were started as indicated in Table 1.

Each experiment was terminated by allowing the DQCM and IRE to warm slowly to 25°C . Subsequently, the LN_2 shroud was also allowed to warm to room temperature. Then, the system was once again backfilled with dry nitrogen, the IRE was removed, and an IR spectrum was taken. It was assumed that the contaminant film on the IRE was representative of the film formed at low temperature. This assumption may be justified somewhat by noting that (1) the more volatile material deposited first, (2) the first several layers of an adsorbed film is difficult to remove even by thermal treatment, and (3) the irradiated condensate, which undergoes less re-evaporation when warmed, has a similar IR spectrum to that of the unirradiated condensate. Total mass loss of the specimen was determined by simply weighing the sample on an analytical balance (± 0.5 mg) before and after the experiment.

Table 1. VCM Facility Outgassing Conditions

Experi- ment	Material	Specimen			Outgassing Time, hr	Target UV Irradiated
		Mass, g	Thickness, 10 ⁻¹ cm	Temp, °C		
1	RTV-615	0.5702	1.10	23	60.0	
				100	120.8	
2	RTV-615	0.5342	1.03	23	96.7	
3	RTV-615	0.5369	1.04	100	24.3	
4	RTV-615	0.5030	0.973	100	111.8	Collectors ^a
5	RTV-615	0.4657	0.900	100	64.3	
6	RTV-615	3.1279	6.05	100	37.7	Collectors ^b
7	RTV-615	0.5306	1.03	100	65.2	Collectors ^b
8	RTV-615	0.5577	1.08	100	114.7	Source ^b
9	RTV-566	1.3018	1.70	100	95.3	Collectors ^b
10	Kapton	0.0563	0.076	23	24.0	

^aIrradiation started during VCM collection.

^bIrradiation started at t = 0.

IV. THEORETICAL CONSIDERATIONS

It is necessary to delineate the relationship between the mass of material as collected on the DQCM and the total VCM emitted by the source. For this purpose, equations were derived by analogy to the field of illuminating engineering.¹⁵ Derivation of the equations are given in some detail because previous derivations of similar relationships were either superficial or did not apply to the present geometry.¹⁶

The quantity of material emitted at an angle θ , M_θ , is related to that emitted perpendicular to a planar outgassing source, M_p , by Knudsen's cosine law:

$$M_\theta = M_p \cos \theta \quad (1)$$

However, to relate the mass per unit area on the DQCM $[(m/A)_{DQCM}]$ to the total VCM, M_T , a relationship between M_T and M_p must be established. Consider first the situation where the DQCM is affixed to the inside surface of a hemispherical cup that encloses the outgassing source at its center (Fig. 5). If the source to collector distance R is assumed to be sufficiently large, then to a first approximation, one may write, from the inverse square law,

$$\left(\frac{m}{A}\right)_{DQCM} = \frac{M_p \cos \theta}{R^2} = \left(\frac{dm}{dA}\right)_{DQCM} \quad (2)$$

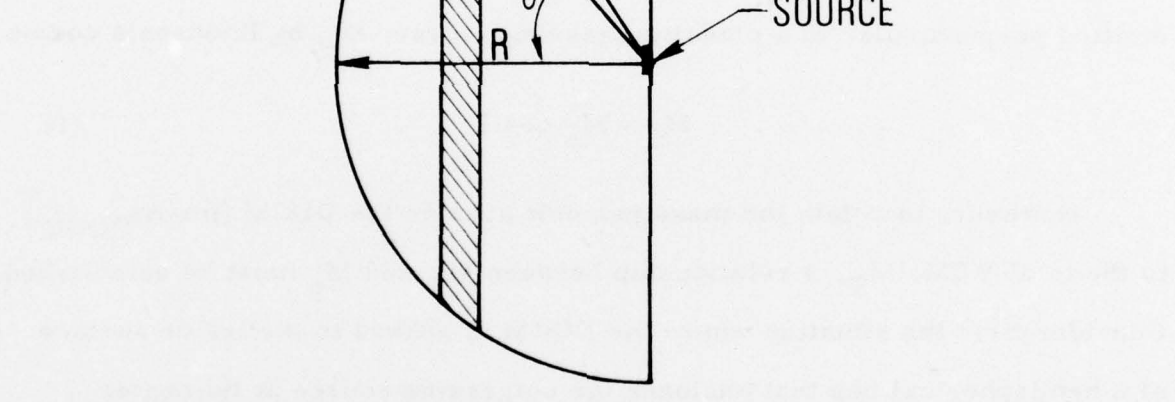


Figure 5. Geometrical considerations for solving relationship of M_T to M_F

Now by integrating the total mass deposited over the available hemispherical surface, one can relate M_T to M_p , i.e.,

$$M_T = \int_0^m dm = \int_0^A \frac{M_p \cos \theta dA}{R^2} \quad (3)$$

The standard method of evaluating this integral is to consider dA as the area confined to a ring of width dl and of radius $R \sin \theta$ (Fig. 5). Since $dl = R d\theta$ and the circumference of the ring is $2\pi R \sin \theta$

$$M_T = 2\pi \int_0^{\pi/2} M_p \sin \theta \cos \theta d\theta = \pi M_p \quad (4)$$

In order to calculate $(m/A)_{DQCM}$ for the case where the source and the DQCM are nonparallel (Fig. 6), an angle correction ψ (the angle between the normal to the DQCM surface and the radius R) must be used. Again, R is large relative to the dimensions of the source. In this case, substitution of M_T/π for M_p in Eq. (2) and multiplication by $\cos \psi$ to take into account the collector angle dependency, yields

$$\left(\frac{dm}{dA}\right)_{DQCM} = \frac{M_T \cos \theta \cos \psi}{\pi R^2} \quad (5)$$

For a source size that may be comparable to R , the relationship between $(dm/dA)_{DQCM}$ and M_T is found as follows.

In the case of a large disk source, the disk is divided up into a series of concentric rings such that each ring has an area of $d\sigma = 2\pi x dx$ (Fig. 7).

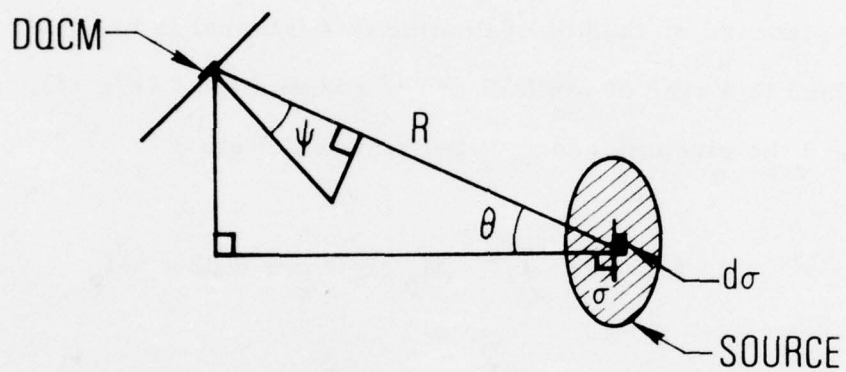


Figure 6. Geometrical considerations for solving relationship of mass on DQCM to M_T when source and collectors are nonparallel

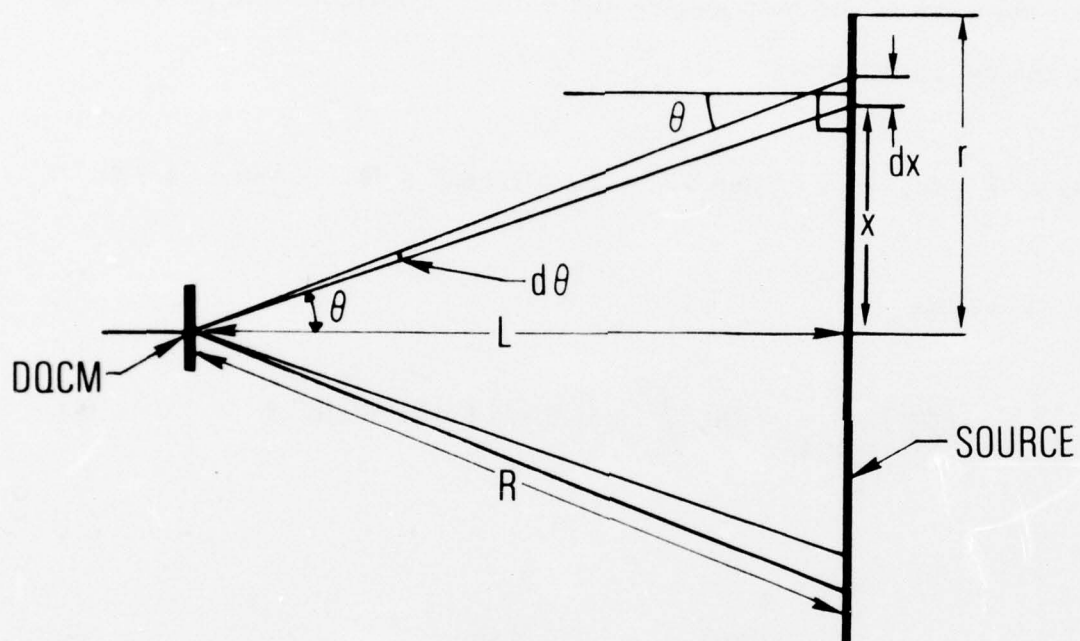


Figure 7. Geometrical considerations for solving relationship of mass on DQCM when source is large relative to collector-source distance

For each disk, R is once again large relative to the dimensions of the source, therefore Eq. (5) applies. Now, $M_T = M\sigma$, where M is the mass emitted from the source per unit area, and σ is the total surface area of the source.

For the case where both source and collector surfaces are parallel and coaxial, the substitution of

$$\sigma = \int_0^\sigma d\sigma, \quad x = L \tan \theta, \quad dx = L \sec^2 \theta d\theta, \quad \text{and} \quad \psi = \theta$$

into Eq. (5) yields

$$\left(\frac{dm}{dA}\right)_{DQCM} = 2M \int_0^\theta \cos \theta \sin \theta d\theta = M \sin^2 \theta \quad (6)$$

or

$$\left(\frac{dm}{dA}\right)_{DQCM} = \frac{M r^2}{r^2 + L^2} \quad (7)$$

From the relationship $M = M_T/\sigma$, and the fact that σ is the area of the source, i.e., πr^2 , $M = M_T/\pi r^2$ can be substituted into Eq. (7). Since $L^2 \gg r^2$ for this facility ($L = 17.4$ cm, $r = 1.27$ cm), then

$$\left(\frac{dm}{dA}\right)_{DQCM} = \frac{M_T}{\pi L^2} \quad (8)$$

It can be shown, by consideration of Knudsen's law, that the distribution of condensate on the DQCM was uniform to within 0.04% (active electrode area ~1 cm). Thus, $(dm/dA)_{\text{DQCM}}$ may be replaced by $(m/A)_{\text{DQCM}}$; hence,

$$(m/A)_{\text{DQCM}} = M_T / \pi L^2 \quad (9)$$

for the VCM facility described herein.

V. RESULTS AND DISCUSSION

A. VOLATILE CONDENSABLE MATERIAL (VCM) AND TOTAL MASS LOSS (TML)

The experimental conditions and results for the three samples tested (RTV-615, RTV-566, and Kapton) are given in Tables 1 and 2. The VCM, given in units of milligrams per steradian, was calculated by multiplying the observed mass per unit area on the DQCM by the square of the source-to-collector distance, i.e., $(m/A)L^2$. Equation (9) derived in the preceding section was used to calculate the total volatile condensable material (TVCM) emitted from the source. The percent volatile condensable material remaining on the DQCM after the collectors were warmed from -140 to 23° C is given in the last column of Table 2.

For the RTV-615 samples, a near mass balance existed between the total emitted VCM as calculated by Eq. (9) and the total mass loss (TML) of the sample. This indicates that little, if any, noncondensable material was emitted by these samples. It also implies that the theoretical derivation is fundamentally correct. Low collection efficiencies (i.e., low TVCM/TML ratios) observed in experiments 2 and 3 resulted from the source being exposed to extended vacuum or heat following the DQCM measurements or both. In particular, experiment 2 was similar to experiment 1 in that the source was heated serially at 23° C and then at 100° C. Loss of coolant in the cryoshield during the second portion of experiment 2 precluded VCM measurements when the source was heated. Therefore, only the 23° C VCM results are

Table 2. Outgassing Results

Experiment	Total Mass Loss		Collected Volatile Condensable Material, mg/sr		Total Volatile Condensable Material, a		Collection Efficiency, %	Contaminant Remaining After Warming, g/b
	mg	%	24 hr	Total hr	24 hr	Total hr		
1	9.0 ± 0.5	1.7	0.58 ^c 1.86 ^d	0.843 2.60	1.83 5.86	2.65 8.17	27 82	7
2	8.3	1.6	0.337	0.66	1.06	2.06	25	2
3	7.7	1.4	1.22	1.41	3.84	4.43	58	4
4	9.1	1.8	2.20	2.52	6.93	7.91	87	65
5	8.1	1.7	2.28	2.63	7.15	8.27	102	
6	15.5	0.50	4.19	4.67	13.2	14.7	95	
7	9.6	1.8	2.59	2.90	8.14	9.15	95	92
8	7.6	1.4	2.02	2.26	6.36	7.11	94	34
9	2.8	0.22	0.226	0.31	0.711	0.97	34	<1
10	0.2	0.36	0.157	0.25 ^f	0.492	0.78	388	<1

^a Calculated (see text).^b Volatile condensable material remaining on the DQCM after warming to 23° C.^c Source at 23° C.^d Source at 100° C.^e Extrapolated value, assuming no irradiation.^f Source at 23° C for 5.33×10^3 min then 100° C for 3.02×10^3 min.

presented. However, the sample continued to lose mass during the 100° C heating period, and this resulted in the low collection efficiency. The collection efficiency given for experiment 2 is nevertheless correct for the portion measured because almost the same ratio was obtained for the first part of experiment 1.

The high collection efficiency observed for Kapton (experiment 10), can be readily explained by the inherently large error in TML. A collection efficiency greater than 100% indicates that more mass was emitted and collected as VCM than was found by weighing the specimen before and after the outgassing experiment. Apparently, absorbed atmospheric gases lost as VCM from the specimen are rapidly regained on subsequent exposure to the atmosphere.¹⁷ Thus, the measured TML value is too low, and consequently the collection efficiency becomes higher than physically possible.

The low collection efficiency observed for RTV-566 appears to be a result of a relatively high level of noncondensables. A 0.22% TML value for the RTV-566 compares favorably with values of 0.23% and 0.27% reported by others for a similar RTV-566.¹⁸ However, this agreement may be more fortuitous than real (see discussion below).

TVCM percentage values calculated for the three samples tested fell within the expected range of values reported by others, i. e., 1.54% (experiment 5), 0.055% (experiment 9), and 0.88% (experiment 10) versus 0.83%, 0.0 to 0.03%, and 0.03%, respectively.¹⁸ (Percent TVCM was calculated by dividing column 6 of Table 2 by column 3 of Table 1 and multiplying by 100.) The higher levels of TVCM in the present experiments may not be only a

consequence of the lower collection temperature (-140°C versus 25°C), they may be due also to differences in sample geometry, as discussed later.

Studies were conducted primarily with RTV-615 because it was readily obtainable and had a sufficiently large outgassing rate that changes due to differing conditions could be observed. Unless stated otherwise, the discussion here concerns the RTV-615 samples. A typical outgassing curve for this material is shown in Fig. 8. It must be pointed out that substantial amounts of material were still outgassing and depositing as VCM for times greater than 24 hr (14.4×10^2 min) at both -140 and 23°C collection temperatures. These results tend to contradict the conclusions made by Muraca and Whittick that nearly all the VCM is collected in 24 hr from 100 to 200 mg samples.³ Their conclusions were made on the basis of large-scale outgassing tests called macro VCM tests, as opposed to the former micro VCM tests, with 4 to 10 gm samples. Their macro TML values are not only greater than the micro TML values, in one case by almost 1000%, but the large samples continued to significantly outgas beyond the 24-hr period (Table 3).

The only agreement between the two tests appears in the TVCM values at or near the detection limit of 0.01%, where round-off errors tend to mask differences. One would have expected the macro TVCM to increase as the macro TML increased because, with time, the outgassing material becomes progressively less volatile and thus tends to be collected more efficiently.

Meaningful TML values can only be given if the source geometry is also specified. In Tables 1 and 2, it is evident that, in the case of RTV-615,

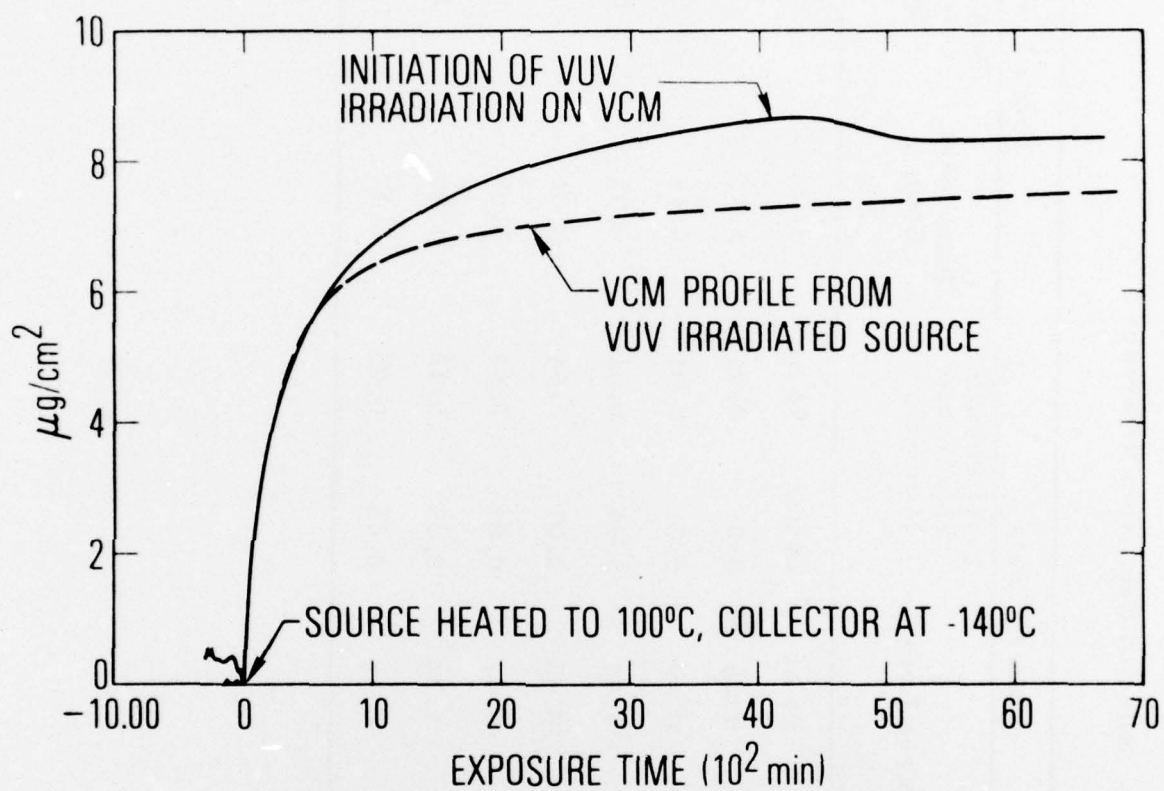


Figure 8. VCM deposition profiles of RTV-615.
— experiment 4; --- experiment 8.

Table 3. Selected Data from Reference 3

Sample	Macro Tests			Micro Tests		
	Total Mass Loss, %	24 hr	96 hr	24 hr	96 hr	24 hr
				Total Volatile Condensable Material, %	Total Volatile Condensable Material, %	Total Volatile Condensable Material, %
Epoxi Patch A/B	0.70	0.70	1.16	0.01	0.01	0.01
Micarta 65M25	0.36	0.36	0.44	0.01	0.01	0.00
Teflon FEP 500 A	0.01	0.01	0.01	0.01	0.01	0.05
Eccofoam S	0.21	0.21	0.48	0.01	0.01	0.07
Delrin 150NC10	0.20	0.20	0.37	0.01	0.02	0.06
Hycar 520-67-108-1	1.19	1.19	1.24	0.10	0.12	0.17
Mystik 7452	0.15	0.15	0.18	0.06	0.05	0.04

an increase in the thickness of the outgassing source from 0.103 cm to 0.605 cm (experiments 6 and 7) decreased the 24-hr TML from 1.61 to 0.44%. A priori, one might have expected the same TML value regardless of sample thickness. The 24-hr TML percentage values were calculated from the ratio of the collection efficiency (column 8, Table 2), the absolute value of the TVCM at 24-hr (column 6, Table 2), and the source mass. Although similar results, i.e., 1.8 versus 0.5%, could have been found in column 3, different outgassing times for the two samples would perhaps have biased the foregoing conclusion. It must be emphasized that most of our samples were equal to or thinner than 0.3 cm, which was the upper limit thickness for the micro tests of Muraca.

On the basis of our experiments and our reinterpretation of the data of Muraca and Whittick,³ we believe that VCM can significantly outgas beyond the 24-hr period, and that the rate of outgassing is diffusion controlled even for micro samples. It is evident that a sample with a high surface-to-volume ratio will outgas far more rapidly than a sample of similar composition with a low surface-to-volume ratio, because, in the latter case, the outgassing molecules have further to diffuse than in the former. Thus, sample mass should be normalized to a given surface-to-volume ratio in calculating TML and TVCM percentages. This outgassing process will be treated in greater detail in a subsequent paper.

B. RADIATION EFFECTS

When vacuum ultraviolet (VUV) irradiation ($\lambda = 184.9$ nm) of the condensate was initiated after collection had already begun, the mass first decreased

and then leveled off (Fig. 8). The decrease in mass was attributable to loss in volatile components caused by photodissociation of the condensate. No significant effects on the VCM deposition profile were observed, however, when the irradiation was started at the same time as the collection (Fig. 9). In this case, the rate of deposition swamped out any small photodissociation effect. It should be noted that when the source was rapidly cooled to -196°C , the VCM curve immediately flattened out, which indicates that outgassing had ceased. The latter observation verifies that background VCM levels were negligible.

In contrast to the case where the condensate had not been irradiated, the DQCM did not return to near its base frequency upon warming to room temperature (Table 2). Apparently, the condensate was fixed to the surface at the low temperature by the VUV radiation through polymerization and cross-linking. Visually, the irradiated VCM appeared as a dark square (unirradiated VCM was transparent). Cross-linking reactions were inferred from the broad IR bands and the relative insolubility of the condensate. Darkening and fixing of condensate by solar irradiation were also noted on recent Skylab flights.¹⁹

The foregoing observations have important implications for the common practice of heating low-temperature critical surfaces to drive off spacecraft contamination. Polymers useful for spacecraft where surfaces are maintained at 25°C or above may be unsatisfactory for those systems that use low temperatures, particularly in cases where such surfaces may be exposed to solar irradiation.

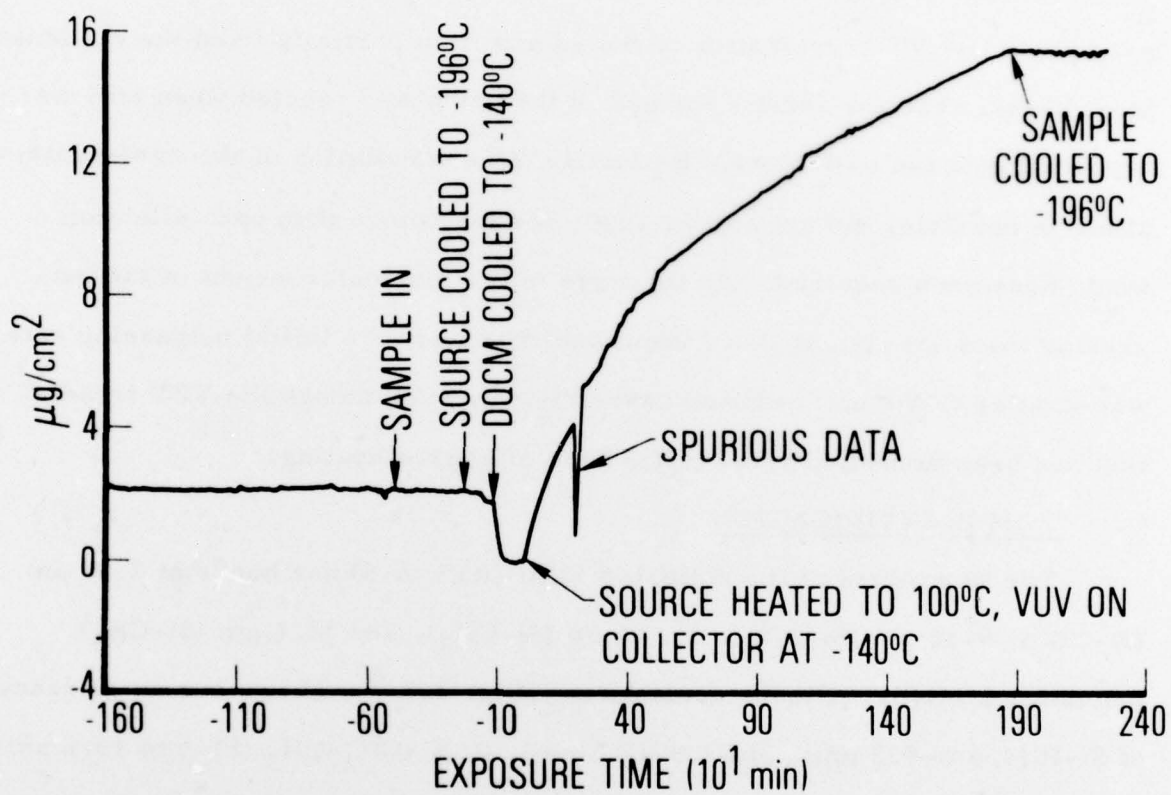


Figure 9. VCM deposition profile of RTV-615 when collectors were irradiated by VUV

VUV irradiation of the specimen resulted in the reduction of long-term VCM (Fig. 8). Apparently, the radiation further cross-linked the cured RTV-615. This had the combined effect of reducing the diffusion rate of the VCM from the host material as well as reducing the vapor pressure of the polymer. The VUV irradiation of the source also partially fixed the condensate. Most likely, reactive radicals formed in the gas phase reacted when they were deposited onto the collectors. Reflective VUV irradiation of the condensate, although possible, did not appear likely because more than one reflection would have been required. An increase in the molecular weight of the outgassing material also appears improbable because the initial outgassing rate was similar to the unirradiated case (Fig. 8), even though the VUV irradiation had been turned on prior to the time of source heating.

C. VCM IDENTIFICATION

The IR spectra of the collected VCM (RTV-615) had bands at $7.93\text{ }\mu\text{m}$ (Si-CH_3), $9\text{--}10\text{ }\mu\text{m}$ (Si-O-Si), $11.75\text{ }\mu\text{m}$ (Si-CH_3), and $12.5\text{ }\mu\text{m}$ (Si-CH_3), indicating a methyl silicone contaminant (Fig. 10).²⁰ There was no evidence of Si-H (4.4 to $4.8\text{ }\mu\text{m}$), SiCH_2Si ($7.3\text{ }\mu\text{m}$), or $\text{Si-CH}_2\text{-CH}_3$ (13.5 to $13.6\text{ }\mu\text{m}$) linkages.²¹

Cross-linking of the VCM by VUV irradiation may have occurred by way of scission of the C-H bond in the methyl group with subsequent formation of $\text{Si-CH}_2\text{-CH}_2\text{-Si}$ -structures. This structure has IR absorption bands at 8.85 and $9.5\text{ }\mu\text{m}$, which would tend to broaden the Si-O-Si IR absorption peaks in the 9 to $10\text{ }\mu\text{m}$ region.²² Such broadening was, in fact, observed.

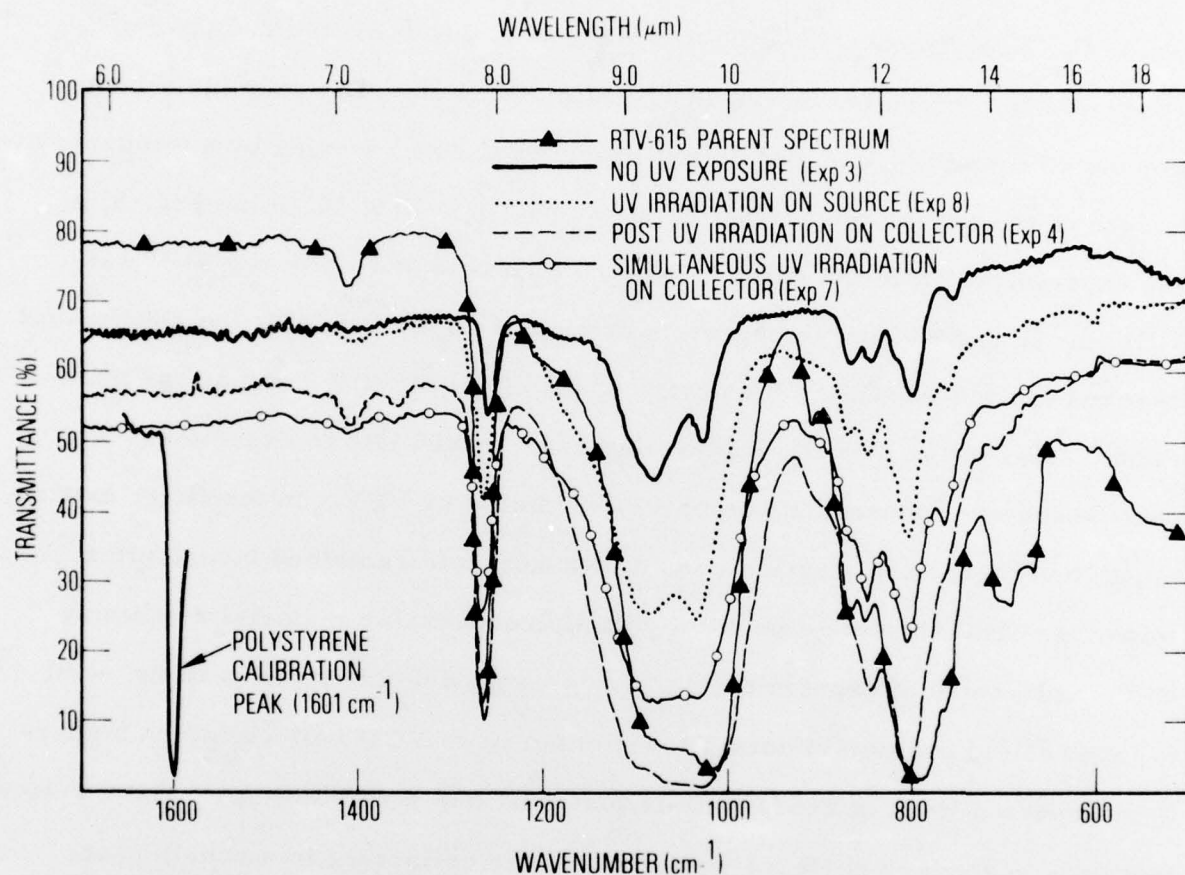


Figure 10. Infrared spectra (25°C) of RTV-615 VCM and RTV-615 parent material

The intensities of the IR absorption peaks were related to the amount of volatile condensable material remaining on the collectors after warming to 23° C. Experiments 3, 4, 7, and 8 had 1.2, 24, 8.9, and 2.5 $\mu\text{g}\cdot\text{cm}^{-2}$, respectively, remaining on the DQCM after warmup. The seemingly large amount of remaining condensate for experiment 4 was caused by a temporary failure of the cryoshield during the latter part ($t > 70 \times 10^2$ min, Fig. 8) of the experiment while the collectors were still cold and while the VUV was still on. In spite of the temporary warming of the cryoshield, the conclusions reached earlier regarding the nature of the effect of VUV irradiations remain valid. Loss of the cryoshield was also experienced late in experiment 3, a case where the condensate was never irradiated by VUV. In the latter experiment, however, only a small amount of condensate remained behind after warming. The absolute amount of volatile condensable material remaining on the collectors of experiment 4 provides a good demonstration of the need for cryoshield protection during low-temperature VCM collection. A higher-than-expected level of condensate is just what one would anticipate for a system that uses secondary surfaces warmer than the collectors in a non-line-of-sight configuration.²

The IR spectrum and, hence, the composition of condensate may be quite different than that of the parent material from which the condensate originated. It should be noted that the IR spectra of the condensate, particularly the spectrum of condensate from experiment 3 in the 9 to 10 μm region, is quite different from that of the parent material in the relative band intensities. Thus, irradiation of deposited VCM, compared with that of thin films

prepared from parent material (pseudo VCM), may yield quite different results and conclusions.²³

Mass spectral analysis of the chamber gases taken with the RGA revealed no significant peaks over and above background levels. The lack of mass spectral peaks may have been a consequence of the non-line-of-sight placement of the RGA relative to the outgassing source. In addition to this possible deficiency, the outgassing levels may have been below the RGA detection limit. Our findings are in agreement with the observations of Goldsmith and Nelson, who also found that cold collectors, because of their time-integrating effect, can detect compounds missed by an RGA.²⁴

VI. CONCLUSIONS

An improved instrument for accurately measuring the rate of contamination from materials under a variety of space environments has been developed. The apparatus is particularly unique because either the outgassing specimen or the condensate may be irradiated in-situ while the collectors are maintained at cryogenic temperatures.

Vacuum ultraviolet irradiation of the cryodeposit from outgassed RTV-615 produces a highly cross-linked condensate that is nonvolatile at room temperature. In the absence of irradiation, however, most of the cryodeposit is sufficiently volatile at room temperature to evaporate. Irradiation of the RTV-615 specimen not only reduces the rate of long-term outgassing but also decreases the condensate volatility.

Specimen geometry rather than mass appears to control the rate at which a sample tends to outgas. Thus, outgassing two specimens of the same composition and of the same weight for a given period of time may lead to widely differing total mass loss and volatile condensable material percentages. This difference results because diffusing molecules will take longer to reach the surface for an outgassing specimen with a small surface-to-volume ratio than for one that has a large surface-to-volume ratio.

PRECEDING PAGE BLANK-NOT FILMED

REFERENCES

1. Rantanen, R. O., Bareiss, L. E., and Ress, E. B., "Determination of Space Vehicle Contamination," Proceedings of Evaluation of Space Environment on Materials, Toulouse, France, June 1974, p. 211.
2. Kan, H. K. A., Journal of Spacecraft and Rockets, Vol. 12, 1975, p. 62.
3. Muraca, R. F., and Whittick, J. S., Polymers for Spacecraft Application Final Report, Stanford Research Institute Project ASD-5046, Jet Propulsion Laboratory Contract No. 950754, Menlo Park, California, 15 Sept. 1967.
4. Method of Test for Total Mass Loss and Collected Volatile Condensable Materials from Outgassing in a Vacuum Environment, ASTM Standard No. E595, American Society for Testing and Materials, Philadelphia, Pennsylvania.
5. Fisher, A., and Mermelstein, B., GSFC Micro-Volatile Condensable Materials System for Polymer Outgassing Studies, NASA-TMX-65399, Goddard Space Flight Center, Greenbelt, Maryland, Oct. 1969.
6. Jensen, L. B., McCauley, G. B., and Honma, M., "Vacuum Thermogravimetric Analysis System for Determination of Continuous Weight Change and Total Condensable Materials," Non-Metallic Materials, Selection, Processing and Environmental Behavior, Vol. 4, Natl. SAMPE Technical Conference Series, Palo Alto, California, Oct. 1972, p. 179.

7. Poehlmann, H. C., "Outgassing and Contamination Properties of Prospective Apollo Telescope Mount Materials," Non-Metallic Materials Selection, Processing and Environmental Behavior, Vol. 4, Natl. SAMPE Technical Conference Series, Palo Alto, California, Oct. 1972, p. 197.
8. Shepherd, J. R., and Corbin, R. L., Review of Scientific Instruments, Vol. 46, 1975, p. 1702.
9. Termeulen, J. Ph., Van Empel, F. J., Hardon, J. J., Massen, C. H., and Poulis, J. A., Progress in Vacuum Microbalance Techniques, Vol. I, Th. Gast and E. Robens, eds., Heyden and Son, Ltd., New York, 1972, p. 41.
10. Niedermayer, R., Gladkick, N., and Hillecke, D., Vacuum Microbalance Techniques, Vol. 5, K. H. Behrndt, ed., Plenum Press, New York, 1966, p. 217.
11. Zelikoff, M., and Aschenbrand, L. M., Journal of Chemical Physics, Vol. 22, 1954, p. 1680.
12. Greiner, N. R., Journal of Chemical Physics, Vol. 47, 1967, p. 4373.
13. Calvert, J. G., and Pitts, J. N., Photochemistry, John Wiley and Sons, New York, 1966, p. 783.
14. Thekaekara, M. P., The Solar Constant and the Solar Spectrum Measured from a Research Aircraft, NASA TR R-351, Goddard Space Flight Center, Greenbelt, Maryland, Oct. 1970, p. 75.
15. Moon, P., The Scientific Basis of Illuminating Engineering, Dover Publications, New York, 1961, Chap. IX.

16. Holland, L., and Steckelmacher, W., Vacuum, Vol. 11, 1952, p. 346.
17. Hait, P. W., The Application of Polyimide to Ultra-High Vacuum Seals, presented 13th National Vacuum Symposium of the American Vacuum Society, San Francisco, California, Oct. 26-28, 1966.
18. Compilation of VCM Data of Non-Metallic Materials, NASA, Lyndon B. Johnson Space Center, Houston, Texas, Apr. 1976, Rev. H.
19. Lehn, W. L., and Hurley, C. J., Results of the Polymeric Films Skylab DO24 Experiment, AFML Technical Report 75-165, Air Force Materials Laboratory, Wright-Patterson AFB, Ohio, 1975.
20. Haslam, J., Willis, H. A., and Squirrel, D. C. M., Identification and Analysis of Plastics, Butterworth and Co., Ltd., London, 1972, 2nd ed.
21. Delman, A. D., Landy, M., and Simms, B. B., Journal of Polymer Science, Vol. 7, Part A1, 1969, p. 3378.
22. Curry, J. W., Journal of the American Chemical Society, Vol. 78, 1956, p. 1686.
23. Fleischauer, P. D., and Tolentino, L. U., "The Far Ultraviolet Photolysis of Polymethyphenylsiloxane Films on Quartz Substrates," Proceedings of the Seventh Conference on Space Simulation, Los Angeles, California, Nov. 12-14, 1973, NASA-SP-336, 1973, p. 645.
24. Goldsmith, J. C., and Nelson, E. R., ASTM/IES/AIAA Space Simulation Conference, Gaithersburg, Maryland, 14-16 Sept. 1970, NBS 336, National Bureau of Standards, Washington, D.C., Oct. 1970, p. 1.

THE IVAN A. GETTING LABORATORIES

The Laboratory Operations of The Aerospace Corporation is conducting experimental and theoretical investigations necessary for the evaluation and application of scientific advances to new military concepts and systems. Versatility and flexibility have been developed to a high degree by the laboratory personnel in dealing with the many problems encountered in the nation's rapidly developing space and missile systems. Expertise in the latest scientific developments is vital to the accomplishment of tasks related to these problems. The laboratories that contribute to this research are:

Aerophysics Laboratory: Launch and reentry aerodynamics, heat transfer, reentry physics, chemical kinetics, structural mechanics, flight dynamics, atmospheric pollution, and high-power gas lasers.

Chemistry and Physics Laboratory: Atmospheric reactions and atmospheric optics, chemical reactions in polluted atmospheres, chemical reactions of excited species in rocket plumes, chemical thermodynamics, plasma and laser-induced reactions, laser chemistry, propulsion chemistry, space vacuum and radiation effects on materials, lubrication and surface phenomena, photo-sensitive materials and sensors, high precision laser ranging, and the application of physics and chemistry to problems of law enforcement and biomedicine.

Electronics Research Laboratory: Electromagnetic theory, devices, and propagation phenomena, including plasma electromagnetics; quantum electronics, lasers, and electro-optics; communication sciences, applied electronics, semiconducting, superconducting, and crystal device physics, optical and acoustical imaging; atmospheric pollution; millimeter wave and far-infrared technology.

Materials Sciences Laboratory: Development of new materials; metal matrix composites and new forms of carbon; test and evaluation of graphite and ceramics in reentry; spacecraft materials and electronic components in nuclear weapons environment; application of fracture mechanics to stress corrosion and fatigue-induced fractures in structural metals.

Space Sciences Laboratory: Atmospheric and ionospheric physics, radiation from the atmosphere, density and composition of the atmosphere, aurorae and airglow; magnetospheric physics, cosmic rays, generation and propagation of plasma waves in the magnetosphere; solar physics, studies of solar magnetic fields; space astronomy, x-ray astronomy; the effects of nuclear explosions, magnetic storms, and solar activity on the earth's atmosphere, ionosphere, and magnetosphere; the effects of optical, electromagnetic, and particulate radiations in space on space systems.

THE AEROSPACE CORPORATION
El Segundo, California

PRECEDING PAGE BLANK-NOT FILMED